Isothermal–isobaric molecular dynamics simulation of polymorphic phase transitions in alkali halides

Imre Ruff
Department of Chemistry, Purdue University, West Lafayette, Indiana 47907

Andras Baranyai
Laboratory of Theoretical Chemistry, Eötvös University, Budapest, Hungary

Eckhard Spohr and Karl Heinzinger
Max-Planck-Institut für Chemie (Otto-Hahn-Institut), Mainz, Federal Republic of Germany

(Received 3 April 1989; accepted 19 May 1989)

As the first application of the isothermal–isobaric molecular dynamics technique to a system with Coulombic forces, the pressure-induced face-centered-cubic to body-centered-cubic transition of some alkali halides is studied assuming Born–Mayer–Huggins potentials between the ions. The long-range forces are handled by the cubic harmonic expansion of the Ewald summation. The property that any periodic boundary condition of orthorhombic symmetry can be uniformly treated in this expansion allows the independent fluctuation of each box length in the course of the simulation of the isobaric ensemble. This reduces stresses during phase transitions from one crystalline state to another and yields less defects. By the appropriate change in the external pressure, the fcc–bcc transition takes place reversibly only in the presence of a considerable amount of defects. Otherwise, quite large hysteresis is found. It is shown that the [100], [010], and [001] directions of the original fcc lattice become the $[\frac{1}{2}\frac{1}{2}\bar{1}]$, $[\bar{1}01]$, and [111] directions in the bcc lattice, respectively. This confirms the Watanabe–Tokonami–Morimoto mechanism supported also by most of the experimental observations.

I. INTRODUCTION

The most simple and widely used algorithms of molecular dynamics (MD) simulations are based on adiabatic (NVE) ensembles. These are convenient to study structural properties of equilibrium systems in which no phase transitions can take place except causing the system to become inhomogeneous in composition or density. On the other hand, since inhomogeneous systems are difficult to handle in the relatively small size of samples under periodic conditions, the molecular dynamics simulation of phase transitions was considerably handicapped as long as only adiabatic ensemble simulations were feasible due to the lack of the theoretical foundation of the canonical (NVT) and isobaric–isothermal (NpT) technique. Although quasicanonical ensembles can be simulated by occasional rescaling of velocities, the simulation is still an adiabatic one between two rescaling regimes of the algorithm. In principle, any exo- or endothermal transition should be studied by carrying out velocity rescaling in every time step, lest the lack of dissipation or supply of heat would prevent transition state configurations to flip over to the next state. Similarly, transformations via transition states requiring an appreciable change in volume would seldom take place in an adiabatic or canonical ensemble simulation within its usual time span.

Although the (NpT) ensemble is, thus, the "natural" ensemble to study phase transitions, F and, the (NpT)-MD algorithm was outlined by Andersen,[1] quite a number of papers have been published partly as methodological improvements,[2–11] and partly as applications to study the properties of liquids,[12–16] it has been applied to phase transitions only in few cases and to simple systems, e.g., Lennard-Jones fluids.[17–20] It was demonstrated in these papers that the freezing–melting transformations can be studied successfully by (NpT)-MD. Thus it can give detailed information on phase transitions on the molecular level. This seems to be one of its main advantages. At the same time, the method is limited to high rates in changing thermodynamic parameters by limitations in computer costs. Yet this may sometimes be an advantage because very high cooling/heating rates are unfeasible in experiments, and so this method is especially suited to study the conditions of crystallization vs glass formation.

However, no phase transitions due to changes in crystal structure have been studied so far by isothermal–isobaric molecular dynamics, in spite of the fact that the considerable activation volume of such a transformation favors the application of this method. In order not to chose artificial models to a study of solid–solid phase transitions, the fcc–bcc (NaCl-type to CsCl-type) transformation of some alkali halides were selected an examples. Namely, some face-centered cubic crystals, stable at room temperature and under normal pressure, can be transformed into a body-centered cubic one by increasing the pressure to a few kbars.[21] Several experiments have been carried out on this kind of first-order transitions mainly on potassium and rubidium halides since its discovery by Slater[22] and various mechanisms have been suggested.[23–26] Theoretical investigations[27] carried out so far are not decisive in favor of one of the mechanisms. Experiments could not get beyond diffraction studies on powders[28] which are not sufficient to prove or disprove the hypotheses.

A study of this kind of phase transitions, however, would require to solve the problem of using long-range Cou-

 0021-9606/89/173148-12$02.10

lombic forces under fluctuating scaling of position coordinates and distances. Therefore, an isothermal–isobaric MD code suited to handle long-range forces was first constructed. This is described in Sec. II. By adjusting the necessary external equilibrium pressure, we attempted to simulate the fcc–bcc transformation of RbBr in both directions with synchronous (Sec. III) and asynchronous fluctuating in the three dimensions of space (Sec. IV) in order to obtain information on the transition mechanism. Results on other alkali halides are summarized in Sec. V.

II. THE SIMULATION METHOD

The pair interactions in alkali halides were modeled by a Born–Mayer–Huggins type of potential with Fumi–Tosi parameters[29]

$$\phi(r_{\alpha\beta}) = \frac{z_\alpha z_\beta e^2}{4\pi\epsilon_0 r_{\alpha\beta}} + A_{\alpha\beta}\exp[B_{\alpha\beta}(\sigma_{\alpha\beta} - r_{\alpha\beta})] - \frac{C_{\alpha\beta}}{r_{\alpha\beta}^6} - \frac{D_{\alpha\beta}}{r_{\alpha\beta}^8}. \quad (1)$$

Since the Coulombic interactions decay slowly, at least this part of the pair potential must be corrected for pairs not directly considered in the simulation box. The usual Ewald summation cannot be trivially generalized to a simulation box fluctuating in length in each direction. The cubic harmonic expansion of the Ewald sum according to Adams and Dubey[30] proved to be a convenient method. Its form is as follows:

$$\psi(\mathbf{q}) = 1/q + \sum_{k=1}^{\infty} A_{2k} C_{2k}(\mathbf{q}) + \sum_{k=6}^{\infty} A'_{2k} C'_{2k}(\mathbf{q}), \quad (2)$$

where the coordinates are measured in units of the box length in the given direction and the constant multiplicator of the Coulomb potential is omitted. In this equation C and C' are terms of the complete orthogonal set of cubic harmonic functions of the form

$$C_{2k}(\mathbf{q}) = \sum_{l=1}^{k} c_{2k,2l} T_{2(k-l)}(\mathbf{q}) \cdot q^{2l}, \quad (3)$$

where

$$T_{2(k-l)}(\mathbf{q}) = x^{2(k-l)} + y^{2(k-l)} + z^{2(k-l)} \quad (4)$$

and the c's are constant coefficients.

Adams and Dubey published optimized A_{2k} coefficients for various number of terms and different box shapes. However, they tested the optimized coefficients by a Monte Carlo program *for the potential and not for the forces.*[30] When we tried to adopt more than seven evenly numbered terms, the forces differed considerably from zero at the surface of the minimum image box which made the simulation unstable. We suspect some typing errors in the $c_{2k,2l}$ coefficients of their C'_{16}, C'_{18}, and C'_{20} terms. Fortunately, the accuracy of the expansion up to the 14th term is satisfactory (errors are less than 1% of the average of the absolute values of the forces), if the A coefficients are optimized as given in Table I.

It is an advantage of the cubic harmonic expansion that it is easily vectorizable and avoids Fourier transformation. Thus, it is mathematically more simple than the method suggested recently.[31]

TABLE I. Optimized coefficients for the cubic harmonic expansion of the Ewald sum.

$2k$	A_{2k}
2	2.943
4	7.762
6	21.83
8	101.69
10	308.56
12	878.0
12′	1027.9
14	3462 0

A further, and even more important, advantage of the cubic harmonic expansion is that it can be easily generalized to a brick-shape simulation box instead of a cubic one. In this way *the three box lengths can fluctuate independently* which may be favorable in phase transitions in the course of which a temporary lowering of symmetry is preferred. For a box of orthorhomic symmetry, the Lagrangian of the system under (NpT) conditions is as follows[17]:

$$\mathscr{L} = \frac{1}{2}\sum_j\sum_i m_i s_j^2 L_j^2 \dot{q}_{ij}^2 - \phi(L_j q_{ij}) + \frac{1}{2} W \sum_j \dot{L}_j^2 - p\prod_j L_j + \frac{1}{2} Q \sum_j \dot{s}_j^2 - (g-1)k_B T \sum_j \ln s_j, \quad (5)$$

where q_{ij} ($i = 1,...,N; j = 1,...,D$) is the coordinate of particle i relative to the box length in the jth direction of the D-dimensional space, r_{ij} the corresponding coordinate on the absolute distance scale, ϕ the potential energy of the particles, s_j the scaling parameter for time (by which kinetic energy and, thus, temperature is kept fluctuating around the value set externally), L_j the box length in direction j, m_i the mass of particle i, g the number of degrees of freedom of the particles, p the external equilibrium pressure, k_B the Boltzmann constant, and T the equilibrium temperature required. The Newtonian equations of motion for this case are obtained from the Lagrangian in the usual way but taking into account that the equidistant time step of the simulation algorithm is compressed or dilated by the s_j parameter. Thus

$$\ddot{q}_{ij} = -\frac{1}{m_i L_j}\cdot\frac{\partial\phi}{\partial r_{ij}} - \left(\frac{\dot{s}_j}{s_j} + \frac{2\dot{L}_j}{L_j}\right)\dot{q}_{ij} \quad (6)$$

for particle motions, while for the "acceleration" of heat transfer we have

$$\ddot{s}_j = \frac{s_j}{Q}\left[\sum_{i=1}^{N} m_i L_j^2 \dot{q}_{ij}^2 - (g-l)k_B T/3\right] + \frac{\dot{s}_j}{s_j}. \quad (7)$$

The form of these equations is independent of dimensionality and the shape of the simulation box which enters only via the equation of motion of the box length (the imaginary pistons pressing the system)

$$\ddot{L}_j = \frac{s_j}{WL_j}\left[\sum_{i=1}^{N}\left(m_i L_j^2 \dot{q}_{ij}^2 - r_{ij}\frac{\partial\phi}{\partial r_{ij}}\right) - pV\right] + \frac{\dot{L}_j \dot{s}_j}{s_j}, \quad (8)$$

where

$$V = \prod_{j=1}^{D} L_j \tag{9}$$

is the volume of the simulation box. The two parameters Q and W are the fictitious masses regulating the frequency of the fluctuations in temperature and pressure. According to our experience stable runs can be achieved by setting them in the order of magnitude of 10^{-21} and 10^{-25} kg, respectively, in agreement with Ref. 17 [notice, however, that in Eq. (8) W replaces the original WV factor].

It is to be emphasized that the essential difference from the original Andersen algorithm is that *the fluctuation of one box length is not coupled directly to the others* (except by the pV term)—similarly to the Parinello-Rahman procedure,[4b] *just as the kinetic energy scaling in a direction is independent from the others* (except the terms containing the desired temperature T)—unlike the procedures of Parinello and Rahman. In its physical meaning this makes the simulation more realistic than that of the original algorithm, since neither the linear expansion nor the velocity of the particles is restricted by some artificial synchronization. With the purpose of comparison, some of our simulations were performed by a synchronous fluctuation of the box lengths according to the original algorithm, but most runs were made allowing brick-shape fluctuations.

It is worth mentioning here in passing that, in addition to their easy vectorizability, the cubic harmonics are suitable to generalize the "Ewald summation" to *any inverse power potential* by differentiating the expansion in Eq. (2) as many times as necessary to obtain $(n-1)!q^{-n}$ in the leading term. This series can be used, after a division by $(n-1)!$, as the expansion of the q^{-n} potential. Although the fast decay of higher order inverse power potentials makes it practically unnecessary in most simulations, these generalizations are equivalent to other methods like that of "shifted forces."[32] According to our tests with 108 Rb^+ and 108 Br^- ions, however, the cutoff error of the non-Coulombic inverse power terms of the Fumi–Tosi potentials was smaller than the small ripples left by the finite-length cubic harmonic expansion. Thus, we used simple minimum image calculations for them.

Our simulations were started from regular lattices with each particle in the local potential energy minimum. Initial velocities were distributed at random according to a Maxwell distribution so that the box, as a whole, neither translated nor rotated. Then the first four steps of the simulation were started by solving the equations of motions by the Runge–Kutta method which produced the necessary "history" of the variables needed for the four-point predictor–corrector routine.[33]

As seen in Eq. (8), the box lengths are controlled by the difference between the kinetic energy on one hand and the sum of the virial and the pV term on the other. In case of crystalline samples *the virial is calculated with some error due to the artificial cancellation of long-range forces at the surface of the minimum image box* around each particle. This error is imposed on the system by the conflicting necessities of having periodic boundary conditions and forces summed up to infinity. Therefore, both the virial and the volume fluctuation controlled by this is more or less erroneous.

For monitoring the changes in local symmetry we used the rotational invariants of the spherical harmonics, or as they are sometimes called, the bond orientational order parameters. They are defined as follows[34–36]:

$$Q_l = \left\{ \frac{4\pi}{2l+1} \sum_{m=-l}^{l} \langle Y_{lm}[\theta(\mathbf{r}),\varphi(\mathbf{r})] \rangle^2 \right\}^{1/2}, \tag{10}$$

where $\theta(r)$ and $\varphi(r)$ are the polar angles of a vector $\mathbf{r}$ (bond) pointing from a given particle to one of its neighbors within a cutoff sphere or selected by some other criterion, Y_{lm} is a spherical harmonic function, and the average of the latter is taken over all bonds. The Q_l's characterize the cosine distribution of angles between pairs of bond vectors in all possible combinations. Thus, they give information on the angular correlations within the whole sample as a space group. In this paper we use them in a renormalized form as suggested in Ref. 34.

Recently it was shown that odd-l invariants can also be very useful in characterizing a network of bond vectors if there are different kinds of particles in the system and so the direction of the bond can be distinguished from its opposite one.[35,37] In the case of a lattice with cubic symmetry, there are many antiparallel bonds which makes the odd-l Q_l's cancel. If such a lattice melts, the odd-l invariants assume a finite value as an indication of the loss of correlations within the space group (while some correlations within point groups may still persist). This property would be suitable to distinguish unanimously even temporary increase of disorder such as transitory melting.

III. POLYMORPHIC PHASE TRANSITION IN RUBIDIUM BROMIDE UNDER SYNCHRONOUS FLUCTUATIONS OF BOX LENGTHS

Experimentalists report that potassium and rubidium chlorides, bromides, and iodides transform from NaCl-type face-centered cubic to a CsCl-type body-centered cubic crystals by an audible click when put under a few kbars of hydrostatic pressure.[23–26] The coordination number of oppositely charged ions changes from 6 to 8, respectively, which makes the bcc structure more preferred at higher pressures due to its closer packing. The same transformation has not been observed for Li halides. NaCl can be forced to change crystal form only at much higher pressure ($\sim$300 kbars).[38]

In order to get more insight into these transitions, we first started a simulation of RbBr from an fcc lattice of 216 particles with an unusually small time step of 1 fs to get frequent snapshots of the configurations. The history in temperature, cubic box length, and some significant Q_l parameters are seen in Fig. 1. A sequence of pair correlation functions is given in Fig. 2. By the latter, more conventional, set of information it is revealed that the peaks following the distance relationships of the fcc structure (labeled by arrows "F") disappear gradually, whereas peaks of the bcc distance sequence ("B") appear simultaneously. The same information is provided by the orientational order parameters:

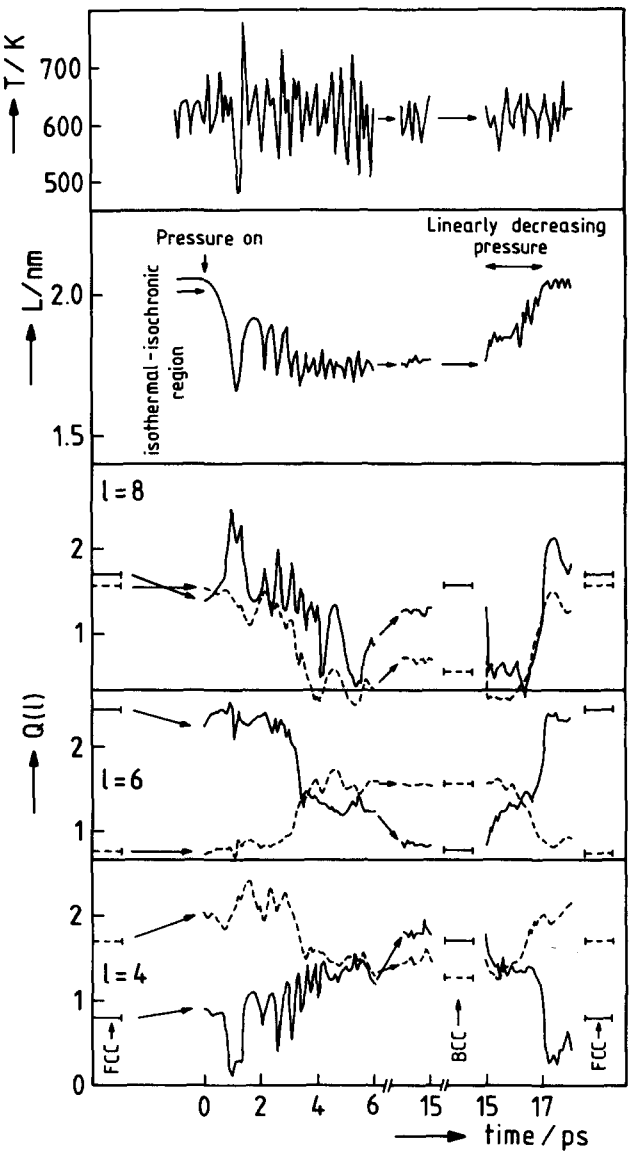

FIG. 1. History of the (NpT)-MD simulation of the fcc–bcc transformation of RbBr. Time is counted from the onset of the high pressure (at the end of an isothermal–isobaric regime). The upper two curves show the temperature fluctuations around 623 K set externally and changes in box length, respectively. The Q_l order parameters are shown for $l = 4$, 6, and 8 (from bottom upwards) and for bonds between the first unlike neighbors (dashed curves) and between first like ones (full curves). On the left- and right-hand side horizontal bars represent the Q_l values corresponding to a regular fcc lattice. Similar bars show those of the bcc lattice after the 15th ps. Transformation occurs between 2 and 4 ps as the sudden changes of the Q_l indicate. Note that unlike-neighbor Q_l's approach their bcc value faster than like-neighbor Q_l's which do it only after considerable annealing (at 14–15 ps). Gradually decreasing the pressure to atmospheric within 2 ps reestablished the fcc structure (see the right-hand side of the graphs).

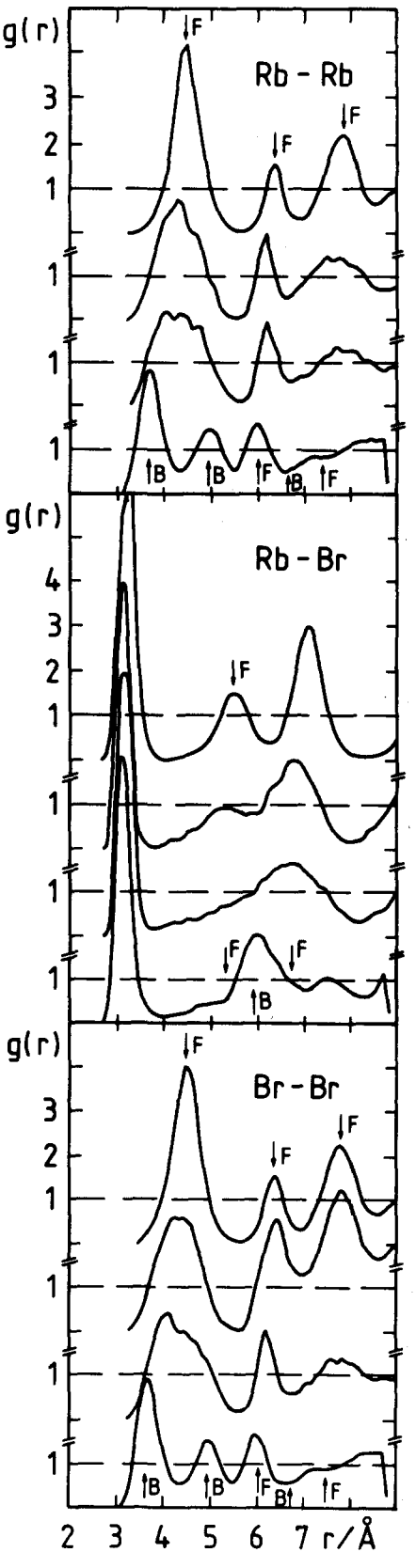

FIG. 2. Variation of pair correlation functions in the course of the fcc–bcc transition. The sequence of the curves from top to bottom in each group corresponds to averages taken in periods prior to onset of pressure, between 0 to 2, 2 to 4, and 13 to 15 ps (after the onset of pressure). Arrows labeled by F and B point to distances expected in a regular fcc or bcc lattice, respectively, if the shortening of distances due to shrinkage during the transformation is accounted for.

Those characterstic of the fcc angular correlation transform gradually into those of the bcc structure.

The set of configurations before and after the phase transition can be used to get decisive information on the detailed mechanism of the transformation. In order to determine the orientation of the crystal with respect to the simulation box, we projected all particles onto the box planes, *xy*, *xz*, and *yz*, and calculated the density maps shown in Figs. 3–5. Cations and anions are mapped separately not to make the graphs too dense. The distinction of their eventual shift with respect to one another is assisted by the polygons drawn inside the frames (a square in the fcc case and other polygons characteristic of the different orientations of the bcc lattice).

The simulation was started from a lattice with the (100), (010), and (001) directions parallel to the axes of the

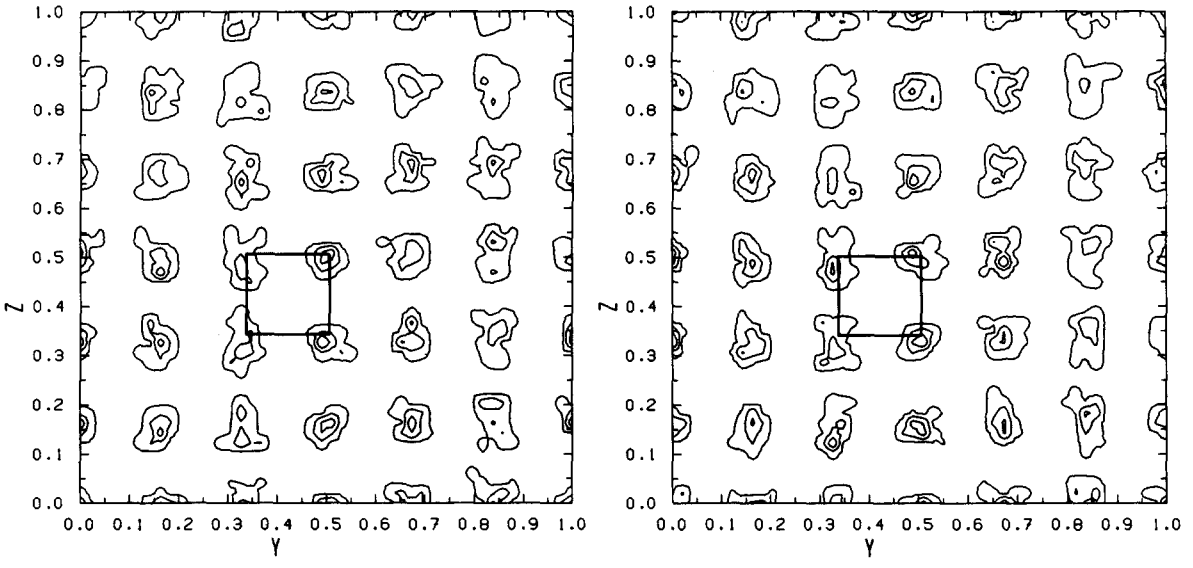

FIG. 3. Density map of the frequency of *yz* coordinates of the fcc lattice before the onset of pressure (left-hand side: Rb^+, right-hand side: Br^-).

simulation box. In Fig. 3 the projections in only one of the spatial directions are shown. Others are very similar to those. The patterns indicate that after the equilibrium runs and the (NpT) regime immediately before the phase transition the orientations were well preserved. The anion and cation spots coincide completely, i.e., there does not seem to be a significant tilt towards any direction.

The projections in the *x* direction shown in Fig. 4 were obtained on configurations between 4 and 6 ps, immmediately after the sudden change in structure. Although disorder is appreciable, a distorted lattice-like order is obvious.

Figure 5 shows the projections in "annealed" configurations between 13 and 15 ps of the history. It is obvious from Fig. 5(c) that the *yz* plane is perpendicular to the (111) direction of a bcc lattice, since one can see the spots arranged in a hexagonal symmetry which is the result of the projection of the vertices of a cube along the three-fold axis. The cations and anions are projected to coinciding positions onto the *xy* plane. By the distance relationship in *x* and *y* direction, and by the requirement that this direction must be perpendicular to (111), one can conclude that Fig. 5(a) is the projection in direction $(\frac{1}{2}\frac{1}{2}\bar{1})$. Consequently, Fig. 5(b) must be the projection in direction $(\bar{1}01)$.

The projections in this latter direction show the highest disorder due to the existence of quite a number of empty channels which, as a matter of fact, is accompanied by several interstitials indicated by the large differences in the line densities of the spots corresponding to occupation densities. In a perfect transformation, each spot in the fcc projection in Fig. 3 should have been split up into two of equal density in

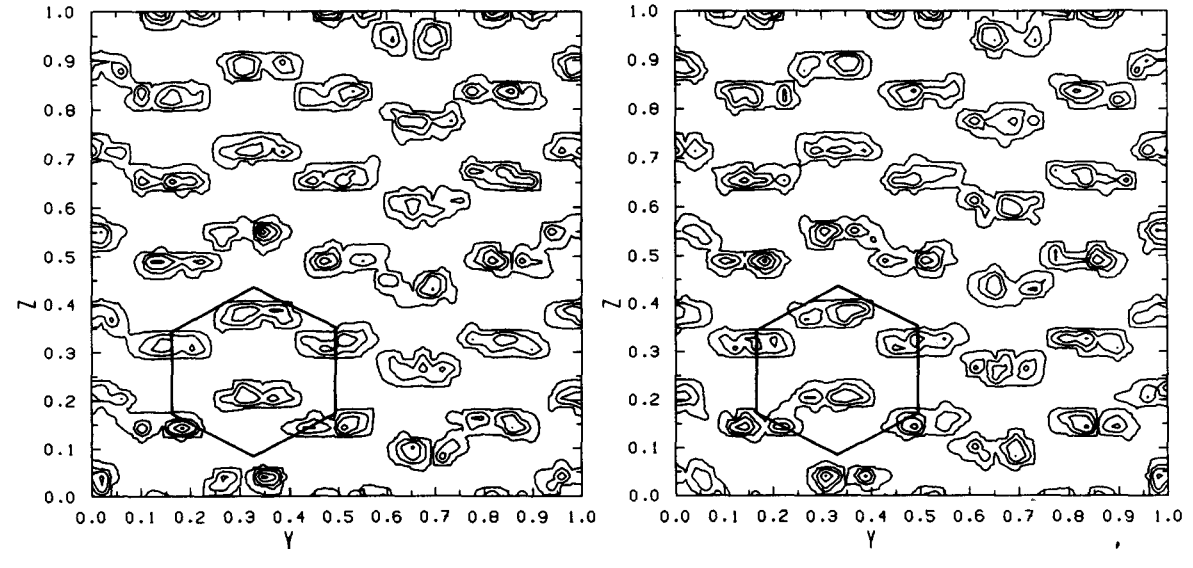

FIG. 4. Density map of the frequency of *yz* coordinates of the lattice between 4 to 6 ps after the onset of pressure (left-hand side: Rb^+, right-hand side: Br^-).

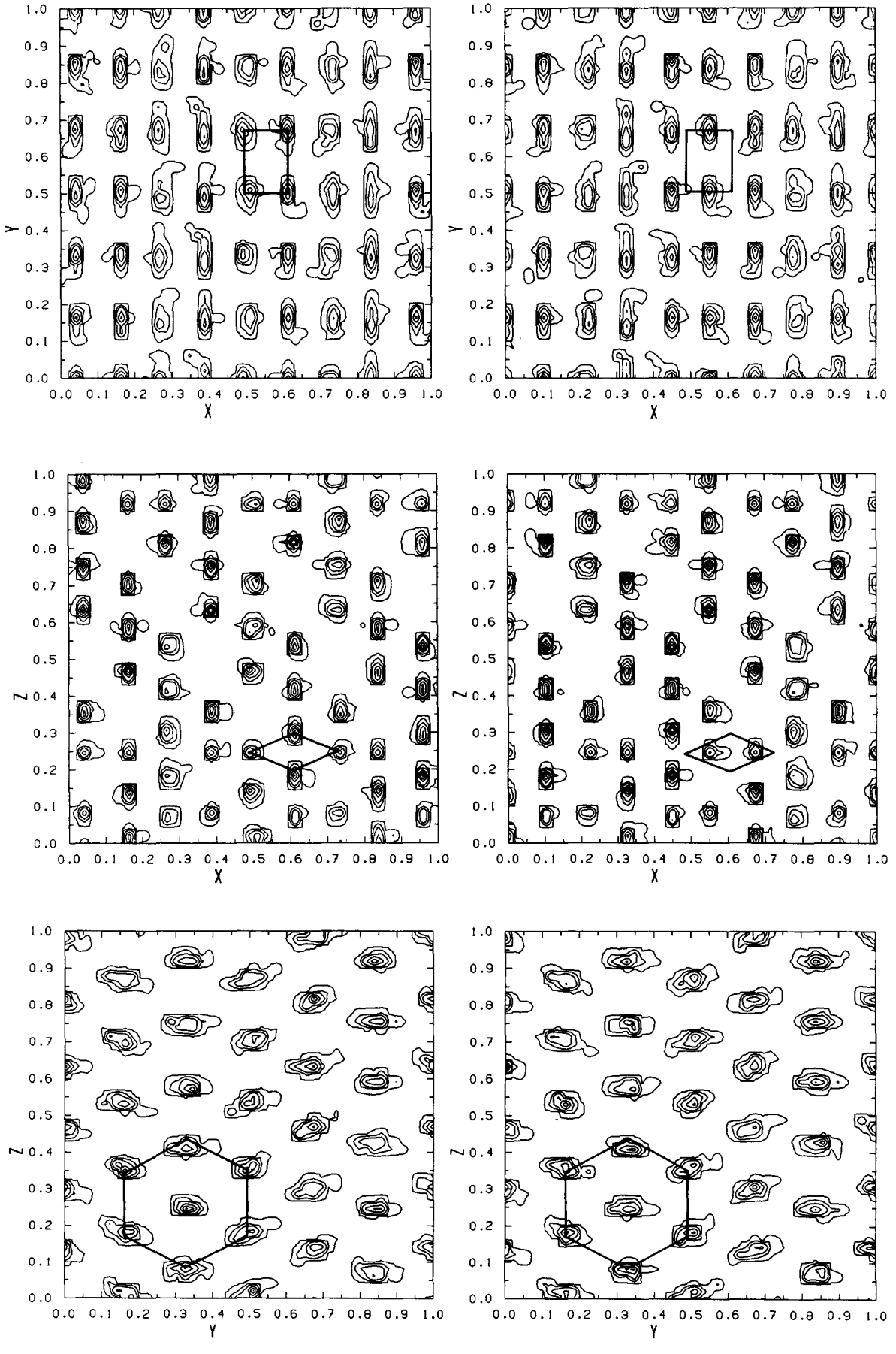

FIG. 5. Density of the frequency of (a) *xy*, (b) *xz*, and (c) *yz* coordinates of the bcc lattice between 13 to 15 ps after the onset of pressure (left-hand side: Rb^+, right-hand side: Br^-).

the ($\bar{1}01$) bcc direction. Instead, some lines of ions corresponding to the spots moved to their new position without splitting up, whereas some lines were left empty. As a result, the bcc lattice contains a high density of defects.

The orientational relationships revealed by these figures confirm the mechanism suggested by Watanabe, Tokonami, and Morimoto[26] *and disprove that of Buerger.*[24]

In order to visualize the mechanism of the transition, we selected three clusters within the cutoff sphere around a Rb^+ whose individual Q_l values were closest to the Q_l averages of all clusters, and followed the change of their coordinates during the transition. Of these, three snapshots are shown in Fig. 6.

The slightly distorted octahedron of bromide ions Nos. 156, 135, 153, 152, 171, and 150 is approached by 138 and 132 from the direction normal to the triangular faces of the octahedron. As a result, the straight line of 156–Rb–150 is tilted to make room for the incoming particles. Finally, 138 becomes part of the cubic coordination sphere, whereas, incidentally, 132 moves away and 173 joins the cluster from an equivalent position of the other side.

With the configurations at hand we could also attempt to analyze some aspects of the lattice dynamics related to this transformation. Although the number of configurations available for the transition state itself is limited by the nature of the process, we used three sets to calculate the velocity autocorrelation functions and the diffusion coefficients as their integral. Diffusion coefficient prior to and after the transformation are in the order of magnitude of 10^{-8} cm^2/s while they increase to 10^{-5} on average over the 2–4 ps range involving the transformation. This indicates considerable displacements during the polymorphic transition.

The reverse transformation was simulated by starting from the end configuration of the fcc–bcc transition and from a regular bcc lattice. In the former case, the decrease of pressure is accompanied by the transition to an fcc lattice with the same orientation as that at the very beginning of the simulation. The projection patterns cannot be distinguished from those in Fig. 3. However, starting from a regular bcc lattice, which underwent an equilibration at 623 K and under high pressure, the release of pressure in the same way as in the former case produced a glassy state. Thus, it seems that the defects play the role of some "memory" facilitating the reversible transition.

IV. POLYMORPHIC PHASE TRANSITION OF RUBIDIUM BROMIDE UNDER ASYNCHRONOUS FLUCTUATION OF BOX LENGTHS

The fcc–bcc transition of RbBr was also studied by letting the box lengths and the instantaneous temperature fluctuate independently in the three spatial directions. This time, however, the change of pressure was not instantaneous but gradual (with a rate of 8.3×10^{15} bar s^{-1}) in order to obtain the minimum pressure at which the transformation takes place.

A part of the history of a run with 216 ions is shown in Fig. 7. It is seen that the three box lengths have to change differently during the transformation: *The crystal shrinks in one direction while expands in the other two,* though not to the same extent. The transition occurs at around 230 kbars which is about 46 times the experimental value. This relatively large error originates from the error of the virial and can be decreased by increasing sample size as will be discussed below.

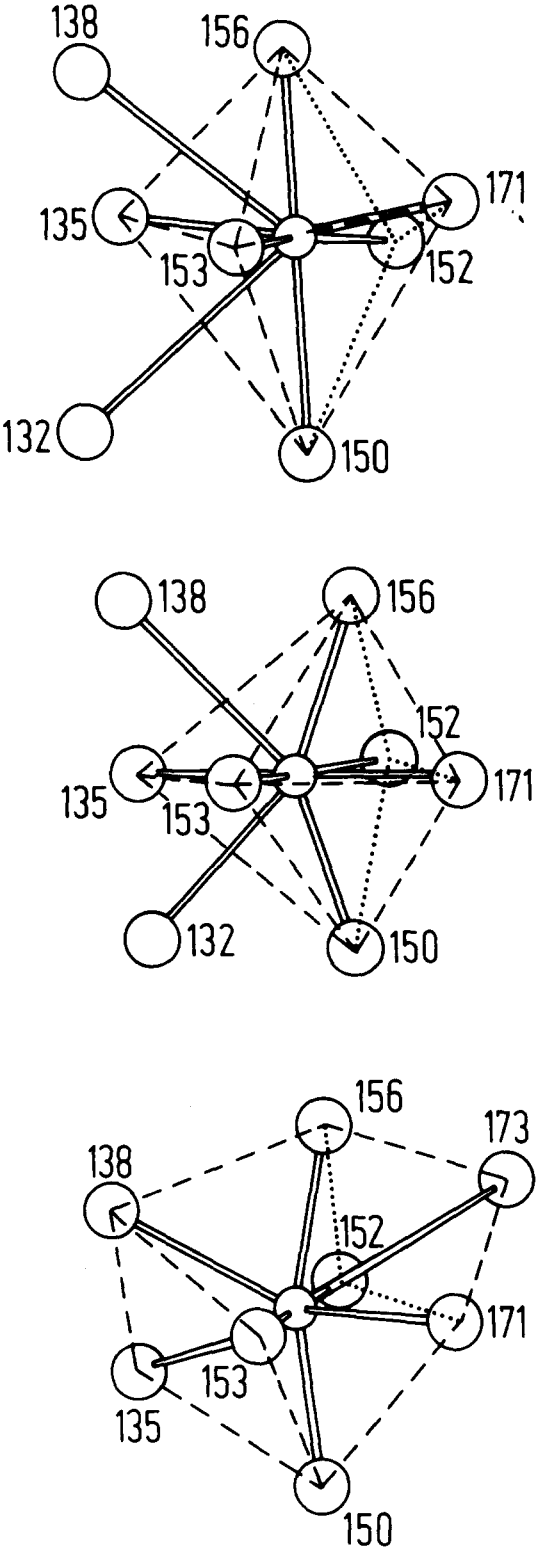

FIG. 6. Snap shots taken of a cluster, having Q_l values close to the average over all clusters, 2.4, 3.1, and 4.0 ps after the onset of high pressure (from top to bottom). The numbers indicate bromide ions.

The changes in the box dimensions can be explained by

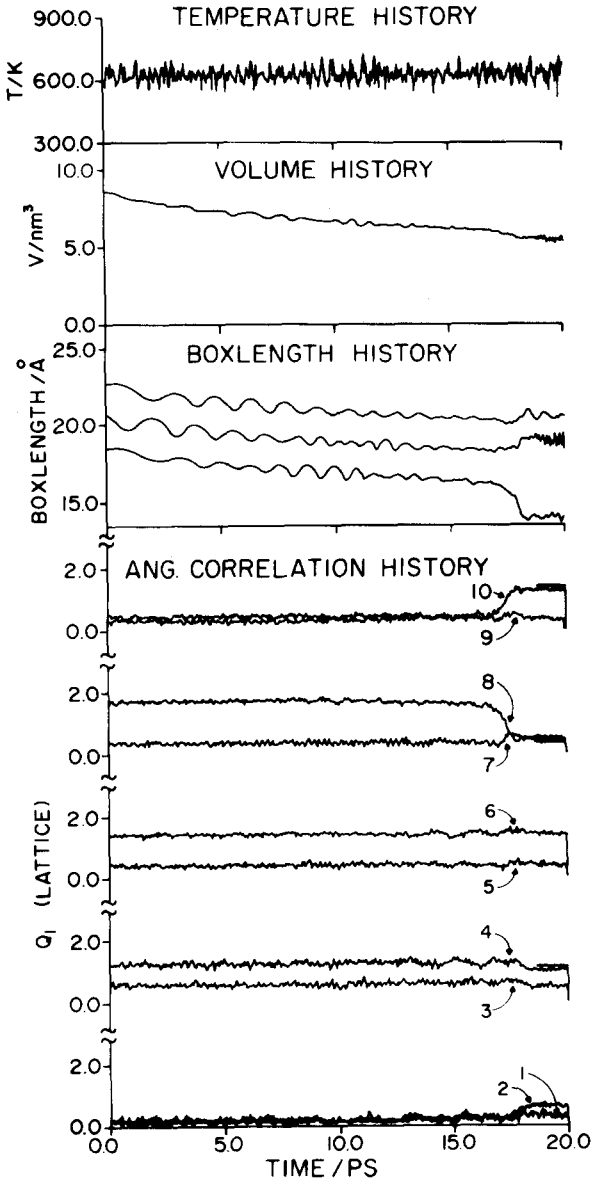

FIG. 7. History of the fcc–bcc polymorphic transition of RbBr under asynchronous fluctuations of box lengths ($N = 216$, $T = 623$ K). Here all Q_l's are shown for $l = 1$ to 10. It is seen that the odd-l order parameters do not increase (not even temporarily) in the transition region. This indicates no transitory melting. On the right-hand side horizontal bars indicate the Q_l values corresponding to regular bcc lattice.

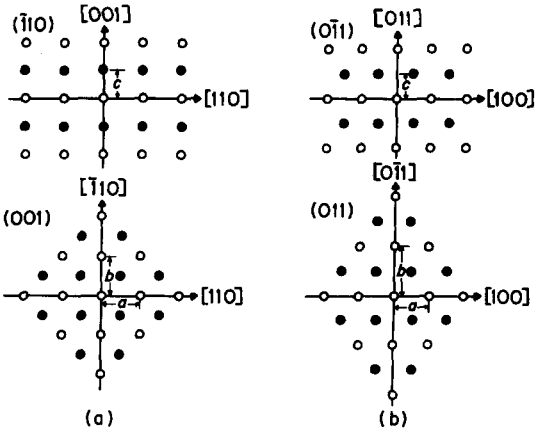

FIG. 8. Schematic representation of the mechanism of NaCl-type (a) to CsCl-type (b) transition.

the requirements of the displacements of crystal layers according to the Watanabe–Tokonami–Morimoto mechanism shown in Fig. 8.[28] The sublattice of a given charge type must move—in a highly collective way—half of an elementary cell length to the [110] direction in order to get eight oppositely charged neighbors instead of six. At the same time, the lattice must be expanded in direction $[0\bar{1}1]$ which, accompanied by an overall decrease in volume, resulted by closer packing, gives less expansion in these directions but more shrinkage in the other.

In Fig. 7 the history of local symmetry is also shown in terms of the changes of order parameters Q_l for $l = 1$ to 10. It is seen that the changes are synchronous with those in box length and volume, and take place within about 2 ps. On the one hand, this is a considerably *faster transformation* than the one obtained with synchronous fluctuation of box lengths, on the other, the transition leads smoothly to Q_l values practically identical with those of the regular bcc lattice.

At the same time the odd-l order parameters remain close to zero throughout the simulation indicating *not even a temporary increase of* nonlattice-like *disorder*. On the basis of this it can be concluded that *the synchronous fluctuation of box dimensions facilitates the polymorphic transition and yields less defects.*

Figure 9 supports this latter conclusion by showing very high regularity in both the [111] and $[\frac{1}{2}\frac{1}{2}\bar{1}]$ directions while in the $[10\bar{1}]$ only a few distortions remained after exactly the same annealing time as that leaving so many defects in the sample shown in Fig. 5.

It is interesting that the remaining defects in the latter direction seem to be dislocations arranged in such a way that some planes form a $>$-shaped structure indicated in Fig. 9(a).

This simulation was repeated with 64, 432, and 512 ions in several runs in order to study the effect of sample size and shape (the 432 sample was a square column made of two 216-atom boxes repeated in the z direction). Figure 10 shows the dependence of transformation pressure as a function of $N^{-1/3}$. The extrapolation of these data to an infinite system is not in contradiction with the experimental value $p_{tr} \cong 5$ kbar. Yet the systematic error in pressure calculation is so large that the simulation has no predictive power in this aspect.

Several attempts have been made to simulate the reverse transformation, viz., the bcc–fcc transition under independently fluctuating box dimensions. Runs were started from regular bcc lattices equilibrated at $T = 623$ K under a pressure of 332 kbar as well as from configurations obtained in previous fcc–bcc transitions. A decrease of pressure at a rate from 8.3×10^{14} to 8.3×10^{16} bar s^{-1} always produced a glassy state whose $g(r)$s were identical with those obtained by cooling the melt to the same temperature.[39] Even this

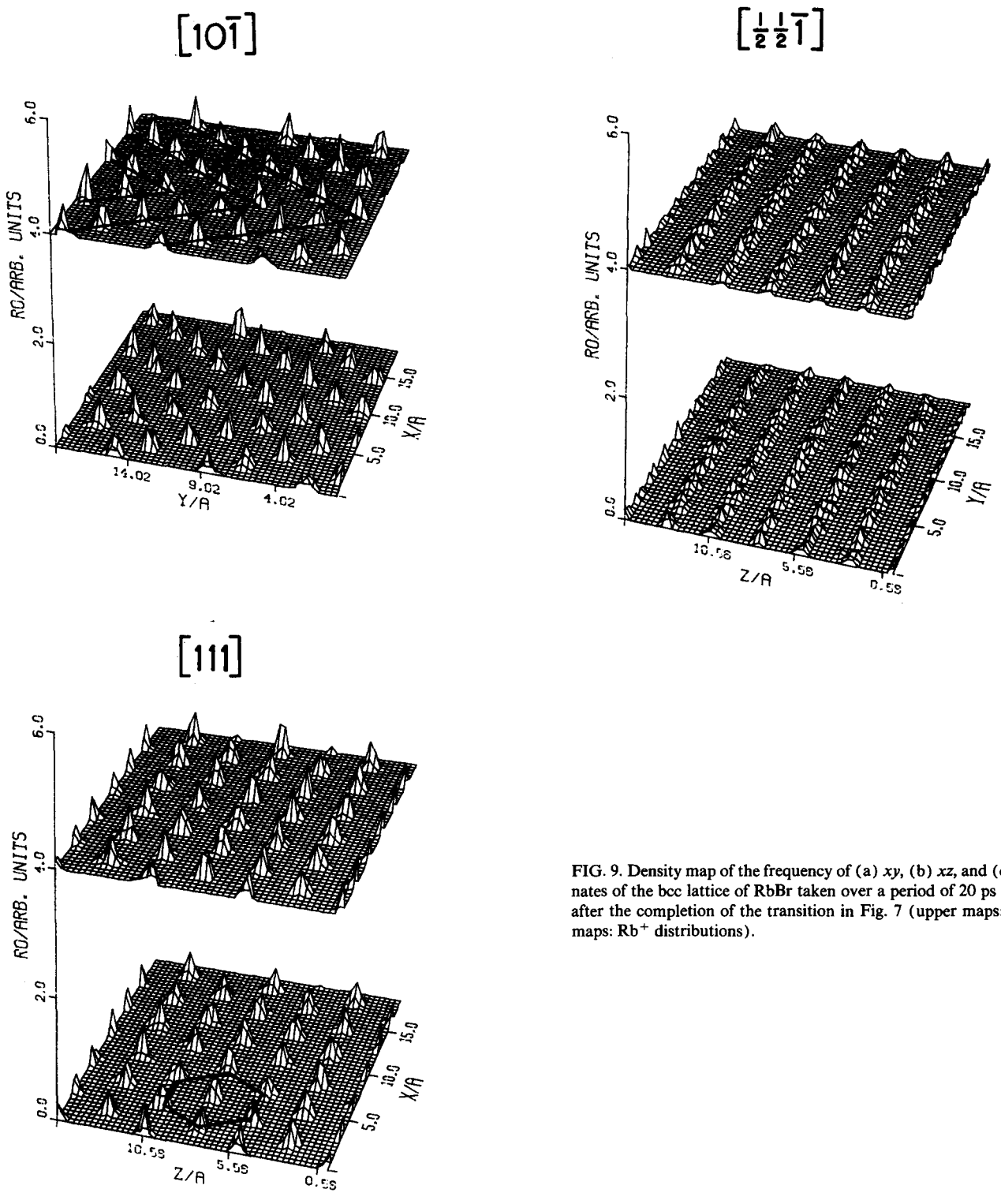

FIG. 9. Density map of the frequency of (a) *xy*, (b) *xz*, and (c) *yz* coordinates of the bcc lattice of RbBr taken over a period of 20 ps immediately after the completion of the transition in Fig. 7 (upper maps: Br^-, lower maps: Rb^+ distributions).

transition was at about 4.1 kbar which indicates a large hysteresis.

Although limitations in computer time do not allow considerably lower rates in pressure reduction and, thus, this phenomenon may be an artifact of the simulation technique itself, it is tempting to assume on the ground of these unsuccessful attempts that the phase diagram is qualitatively similar to Fig. 11, and that increasing pressure at 623 K would take the system out of the region where instability criteria do not prevent glass formation to a region where only the bcc crystal is stable. The reverse route, then, moves the system through a glass transition instead of a transition to the fcc

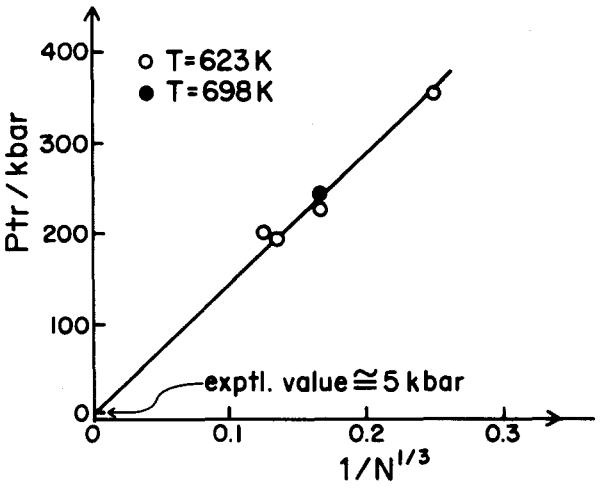

FIG. 10. Extrapolation of the pressure of transformation (p_{tr}) to infinite system.

form. The latter, it seems, can be obtained only in systems containing as many defects as those in the sample discussed in Sec. III.

V. STUDIES ON OTHER ALKALI HALIDES

Table II summarizes the thermodynamic data calculated in (NpT)-MD simulations of some other alkali halide crystals. Comparison with some experimental results show that both molar volume and internal energy data are in very good agreement with experiments. The same is true for isobaric molar heat capacity data which are, as a matter of course, more sensitive to errors originating from the approximate nature of pair potentials since they come from fluctuations. Knowing the systematic error in calculating the pressure due to errors in the virial, it is rather surprising that the isothermal compressibility data are not even worse than those in Table II.

The pressures of the fcc–bcc transformation are listed in Table III. No such transformation could be observed for LiCl in which the ratio of ionic radii seems to prefer the fcc structure even at very high pressures. Further increase of pressure resulted in such large fluctuations that the simulation became instable.

Although the pressure of transformation involves systematic error due to size effects, their sequence in the NaCl–KCl–RbBr series corresponds to what would be expected by simple packing rules based on the ratio of cationic and anionic radii. There is also a size effect in the volume at the transition pressure relative to that under atmospheric pressure. This seems to be a result of larger hysteresis in smaller simulation boxes. Again, extrapolation to infinite system size yields volume shrinkage not in contradiction with experimental data (about 15%).[28]

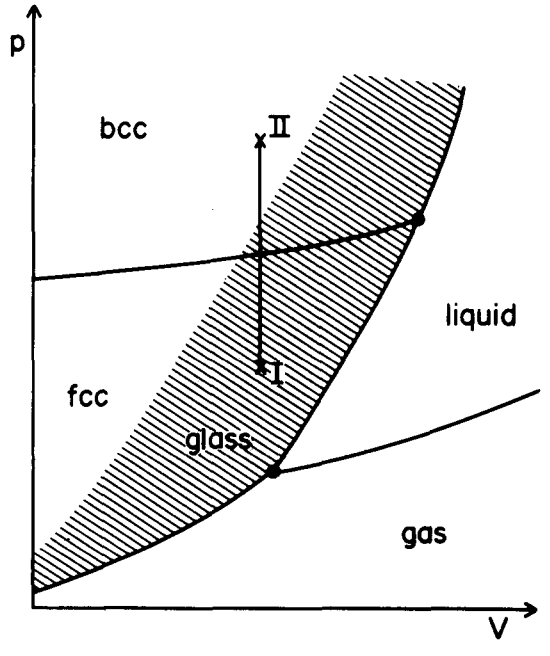

FIG. 11. Schematic phase diagram of an alkali halide. Starting from a regular lattice in point I and increasing the pressure to point II would take the system through a solid-to-solid phase transition. However, lowering the pressure from II would result in a glass transition.

VI. CONCLUSIONS

Our study can be summarized from methodological and physical points of view:

The (NpT)-MD simulation technique has been extended to Coulombic systems in which both the generalization to brick-shape simulation box as well as the computationally advantageous cubic harmonic expansion of the Ewald summation is conveniently applied. By isothermal–isobaric molecular dynamics, the properties and transformations of many-particle systems can be studied under more realistic thermodynamic conditions if fluctuations in both kinetic energy and volume are allowed to be independent in the three directions of space. It is also a methodological result that the orientational order parameters (rotational invariant of spherical harmonics—including odd-l ones—of "bonds" between neighboring particles) proved to be very sensitive indicators of structural changes.

The method has been applied to study polymorphic phase transitions in alkali halide crystals. The simulation of the fcc–bcc transition of NaF, NaCl, KCl, and RbBr reveal details in the molecular mechanism of the geometrical changes of configurations. The transformation takes place throughout in crystalline phase with not even a temporary appearance of a liquid-like disorder. This means that the atomic motions are very collective in nature and there is a real possibility of sliding complete crystal planes to their new positions.

Details of orientational relations between crystal faces prior to and after the transformation proves the Watanabe–Tokonami–Morimoto hypothesis according to which the [100], [010], and [001] directions of the NaCl-type lattice become the $[\frac{1}{2}\frac{1}{2}\bar{1}]$, $[10\bar{1}]$, and [111] directions in the CsCl-type one.

TABLE II. Comparison of calculated and experimental data at 1 bar for some crystalline alkali halides.

		V_m (cm^3)		$-\langle U_m \rangle$ (kJ mol^{-1})	
Salt	N	calc.	expt.	calc.	expt.[a]
LiCl	216	21.6 ± 0.5[g]	20.50[c]	811.9 ± 2.2[g]	829.0
NaF	216	13.7 ± 0.4[g]	16.42[c]	875.5 ± 2.3[g]	···
NaCl	216	28.8 ± 0.3[g]	27.0[c]	739.1 ± 1.5[g]	765.0
KCl	216	39.4 ± 0.4[g]	38.76[g]	671.5 ± 1.5[g]	688.0
RbBr	64	50.2 ± 0.7[g]	51.7[c]	620.8 ± 3.0[g]	641.6
	216	51.3 ± 0.6[g]		622.7 ± 1.5[g]	
	432	50.6 ± 0.4[g]		622.4 ± 0.8[g]	
	512	50.7 ± 0.3[f]		623.4 ± 0.7[f]	
	512	50.8 ± 0.3[g]		622.0 ± 0.8[g]	
	512	53.7 ± 0.5[i]	53.7[h]	600.9 ± 1.5[i]	

		C_{mp} (J mol^{-1} K^{-1})		κ_T (Mbar^{-1})	
Salt	N	calc.	expt.	calc.	expt.
LiCl	216	49.9[g]	54.9[b]	23.4[g]	3.34[g]
NaF	216	60.6[g]	46.8[e]	20.6[g]	2.23[d]
NaCl	216	50.0[g]	51.3[e]	7.2[g]	4.52[g]
KCl	216	46.2[g]	51.3[c]	9.9[g]	5.2[c]
RbBr	64	66.7[g]	52.9[c]	9.4[g]	7.94[c]
	216	45.7[g]		12.7[g]	
	432	49.2[g]		9.2[g]	
	512	55.8[f]		10.9[f]	
	512	46.9[g]		7.0[g]	
	512	53.0[i]		11.8[i]	

[a] $T = 0$ K.
[b] $T = 293$ K.
[c] $T = 298$ K.
[d] $T = 300$ K.
[e] $T = 500$ K.
[f] $T = 598$ K.
[g] $T = 623$ K.
[h] $T = 990$ K.
[i] $T = 998$ K.

Simulations of the reverse transition were successful only if there were many defects in the bcc crystal. Perfect bcc crystals, in contrast, underwent a transition to a glassy state at pressures much lower than that required to the forward transition. Since this observation may be an artifact due to the inherently fast rate of pressure changes in simulations, the reversibility of these polymorphic transitions needs further methodological studies.

TABLE III. Calculated pressure of the fcc–bcc transformation of some alkali halides.

Salt	N	T(K)	p_{Tr} (Kbar)	$V_{bcc,p_{Tr}}/V_{fcc,0}$
LiCl	216	623	> 3500	···
NaF	216	623	815	0.527
NaCl	216	623	1033	0.441
KCl	216	623	531	0.556
RbBr	64	623	355	0.560
	216	623	228	0.641
	216	698	245	0.640
	432	623	196	0.672
	512	623	203	0.687

ACKNOWLEDGMENTS

I. R. and A. B. are grateful to the Hungarian Academy of Sciences for financial support of part of this work under Grant No. AKA-1-3-86-0-163. I. R. is also grateful to the Council of International Exchange of Scholars for the Fulbright Fellowship and to the Max-Planck-Gesellschaft which made most of this work feasible.

[1] H. C. Andersen, J. Chem. Phys. **72**, 2384 (1980).
[2] J. R. Ray, H. W. Craben, and J. M. Haile, J. Chem. Phys. **75**, 4077 (1981); Nuovo Cimento, **64**, 191 (1981).
[3] J. M. Haile and H. W. Graben, J. Chem. Phys. **73**, 2421 (1980).
[4] (a) M. Parrinello and A. Rahman, Phys. Rev. Lett. **45**, 1966 (1980); (b) J. Appl. Phys. **52**, 7182 (1981).
[5] M. Parrinello and A. Rahman, in *Melting Localization and Chaos*, edited by R. K. Kalia and P. Vashishta (Elsevier, Amsterdam, 1982).
[6] R. G. Murro and R. D. Mountain, Phys. Rev. **28**, 2261 (1983).
[7] S. Nosé and M. L. Klein, Phys. Rev. Lett. **50**, 1207 (1983).
[8] D. Levesque, J. J. Weis, and M. L. Klein, Phys. Rev. Lett. **51**, 670 (1983).
[9] J. P. Ryckaert and G. Ciccotti, J. Chem. Phys. **78**, 7368 (1983).
[10] S. Nosé and and M. L. Klein, Mol. Phys. **50**, 1055 (1983).
[11] M. Ferrario and J. P. Ryckaert, Mol. Phys. **54**, 587 (1985).
[12] S. Nosé and M. L. Klein, J. Chem. Phys. **78**, 6928 (1983).
[13] J. M. Haile and S. Gupta, J. Chem. Phys. **79**, 3067 (1983).
[14] H. J. C. Berendsen, H. P. M. Postma, W. F. van Gunsteren, A. Di Nola, and J. R. Haak, J. Chem. Phys. **81**, 3684 (1984).

[15]D. Brown and J. H. R. Clarke, Mol. Phys. **51**, 1243 (1984).
[16]D. M. Heyes, Chem. Phys. **82**, 285 (1983).
[17]S. Nosé, Mol. Phys. **52**, 255 (1984); S. Nosé and F. Yonezawa, J. Chem. Phys. **84**, 1803 (1986).
[18]D. K. Chokappa and P. Clancy, Mol. Phys. **61**, 597, 617 (1987).
[19]F. Yonezawa, S. Nosé, and S. Sakamoto, J. Non-Cryst. Sol. **97-98**, 373 (1987).
[20]F. Yonezawa, S. Nosé, and S. Sakamoto, J. Non-Cryst. Sol. **95-96**, 83 (1987).
[21]P. W. Bridgman, Z. Kryst. **67**, 370 (1928); Pr. Am. Acad. **71**, 387 (1936/37).
[22]J. C. Slater, Phys. Rev. **23**, 488 (1926).
[23]H. Shoji, Z. Kryst. **77**, 381 (1931).
[24]M. J. Buerger, in *Phase Transformation in Solids*, edited by R. Smoluchowski, J. E. Mayer, and W. A. Weyl (Wiley, New York, 1951).
[25]W. L. Fraser and S. W. Kennedy, Acta Cryst. A **30**, 13 (1951).
[26]M. Watanabe, M. Tokonami, and N. Morimoto, Acta Cryst. A **33**, 294 (1977).
[27]R. J. Wallot and J. Baker, J. Phys. Chem. Solid **39**, 1147 (1978).
[28]N. Nakagiri and M. Nomura, J. Phys. Soc. Jpn. **51**, 2412 (1982).
[29]M. P. Tosi and F. G. Fumi, J. Phys. Chem. Solids **25**, 31 (1964).
[30]D. J. Adams and G. S. Dubey, J. Comput. Phys. **72**, 156 (1987).
[31]T. Nguyen, Inf. Quart. Comp. Sim. Cond. Phases, No. 28, p. 48ff, 1988.
[32]F. H. Stillinger and R. A. LaViolette, Phys. Rev. B **34**, 5136 (1986).
[33]Our predictor–corrector program was based on the Adams–Bashforth method with the modification by Adams and Moulton as given in G. A. Korn and Th. M. Korn, *Mathematics for Engineers and Scientists* (Hungarian translation) (Muszaki Kiado, Budapest, 1975) (except two obvious typing errors giving $3f$ instead of $9f$ in the equation for y_{k+1}^{pred}, and y instead of f in the equation for y_{k+1}^{corr}).
[34]A. Baranyai, A. Geiger, P. R. Gartrell-Mills, K. Heinzinger, R. J. McGreevy, G. Palinkas, and I. Ruff, J. Chem. Soc. Faraday Trans. 2 **83**, 1335 (1987).
[35]L. Pusztai, A. Baranyai, and I. Ruff, J. Phys. C **21**, 3687 (1988).
[36]P. Steinhardt, D. R. Nelson, and M. Ronchetti, Phys. Rev. B **28**, 784 (1983).
[37]R. L. McGreevy, A. Baranyai, and I. Ruff, Acta Chim. Hungary **125**, 717 (1988).
[38]A. L. Ruoff (private communication).
[39]I. Ruff (in preparation).